Pete's Thesis

by

Peter Thompson

A thesis submitted in conformity with the requirements
for the degree of Doctor of Philosophy
Graduate Department of Physics
University of Toronto

Abstract

Pete's Thesis

Peter Thompson

Doctor of Philosophy

Graduate Department of Physics

University of Toronto

2011

(At most 150 words for M.Sc. or 350 words for Ph.D.)

Contents

Chapter 1

Introduction

1.1 LHC

1.2 Standard model

Chapter 2

The ATLAS Detector

2.1 Inner Detector

2.2 Calorimeters

2.2.1 Forward Calorimeters

The ATLAS Forward Calorimeters (FCal) are located next to the beampipe, 4.6m away from the ATLAS interaction point on either side. These are liquid Argon based calorimeters, and are located within a special support tube inside the end-cap cryostat (figure 2.1).

The FCal consists of three modules, one electromagnetic module (FCal1) and two hadronic modules (FCal2 and FCal3). Each module has a cylindrical shape, with an outer radius of $450mm$ and a length of $440mm$. A plug made of brass alloy has a similar shape and is located behind the hadronic modules in order to provide additional shielding for the muon chambers behind it. As the FCal operates at a temperature of about 90K in ATLAS, "cold" lengths will be used in the following when quoting dimensions and densities, etc.

The electromagnetic modules of the FCal were produced by the university of Arizona. Each module consists of a number of circular copper plates with an inner radius of X

and an outer radius of x. On one side (the ATLAS "A" side, $z > 0$ in the ATLAS coordinate system), the FCal 1 module consists of 18 plates of thickness 24 mm, whereas on the opposite side (the "C" side) 19 slightly thinner plates are used. Each plate is drilled with a hexagonal array of holes into which the electrodes were inserted. Each electrode consists of a copper tube (the cathode) containing a copper rod (anode) around which a PEEK fiber is wrapped. The Inner diameter of the copper tubes is 2.62 mm while the diameter of the copper rods is 2.35mm, thus leaving a gap of 267 μm which is filled with liquid Argon. The PEEK fiber has a diameter of 250 μm, and is present to keep the rod positioned in the centre of the tube, thus maintaining the uniformity of the LAr gap throughout the electrode. Typical gap sizes used in LAr calorimeters are on the order of a few millimetres, however as the FCal is located at high pseudorapidity minimum bias events will deposit energy in it at a very high rate. The smaller gap size is required in order to reduce the drift time across the gap, and thus preventing the high rate of ionization from causing a build-up of positive ions in the liquid argon. The distance between electrodes in FCal1 is similar to the Moliere radius (a measure of the lateral spread of an electrmagnetic shower) for copper. EM showers in the FCal should thus spread across several electrodes, allowing the calorimeter to sample the shower effectively. Copper also allows the FCal1 module to conduct heat efficiently. This is important, as it prevents the energy deposited within the FCal from raising the temperature of the liquid argon above its boiling point.

The hadronic modules of the FCal were produced at the University of Toronto (FCal2) and at Carleton University in Ottawa (FCal3). Each of these modules uses two copper end plates drilled with a hexagonal array of holes, each of which holds an electrode. The electrodes in these cases use copper tubes for their anodes but rods made of pure tungsten (with density 19.2) for the cathodes. The absorbing matrix is formed from small slugs of tungsten alloy ("WFeNi" - 97% tungsten/2% Iron/1% Nickel) positioned in the gaps between the electrode tubes. The material composition and density of the calorime-

ter components are important factors when defining the geometry of the calorimeter in simulations. By themselves, the WFeNi slugs have a density of 18.3 g/cm^3. When considering the WFeNi slugs, the copper electrode tubes, the tungsten rods and any spaces in the absorber matrix that are filled with liquid argon, the average density of absorbing material in the hadronic modules is 14.33 g/cm^3 for FCal2 and 14.45 g/cm^3 for FCal3 [9]. A diagram showing the way in which the WFeNi slugs are positioned amongst the electrodes is shown in figure 2.2

As charge is deposited in the liquid argon, it drifts due to the electric field present in the electrode, causing a current which is used as a signal. The electronics chain used to read out and process this signal is discussed in detail in section 3.3.

quantity	FCal1	FCal2	FCal3
Absorber material	Copper	Tungsten	Tungsten
Module inner diameter	720 mm	790 mm	860 mm
Electrode Seperation	7.5mm	8.62 mm	9.0mm
Rod Diameter	2.35 mm	2.47 mm	2.75 mm
Tube inner diameter	2.62 mm	2.84 mm	3.25 mm
LAr Gap	267 μm	375 μm	500 μm
distance from IP to front face	4668.5mm	5128.3 mm	5602.8

Table 2.1: Dimensions of the FCal modules.

2.3 Muon Spectrometer

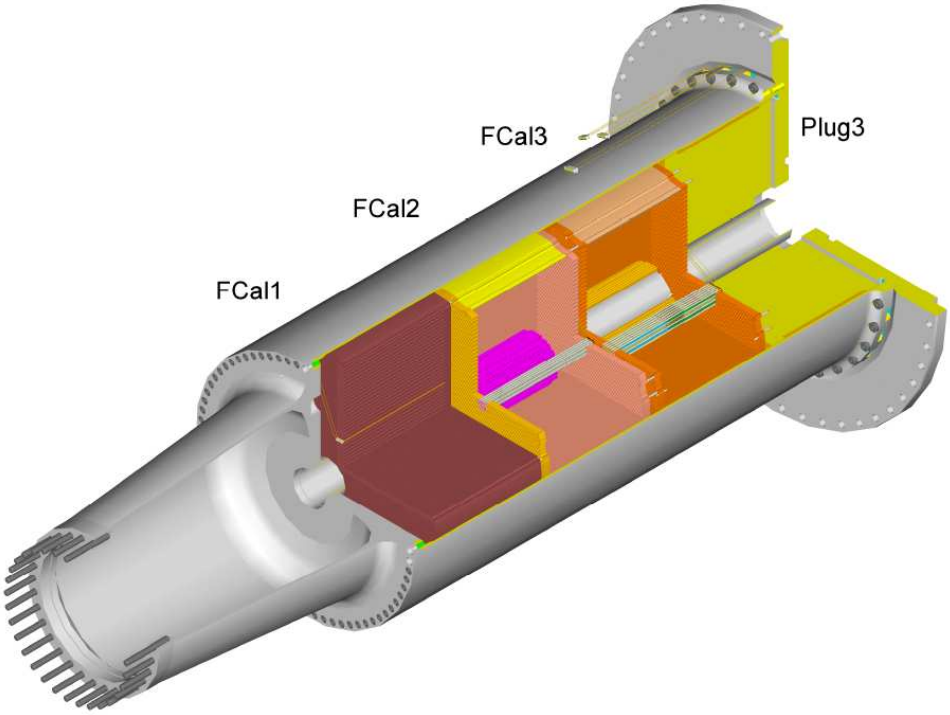

Figure 2.1: Cut-away view showing the FCal within its support tube (taken from [2]).

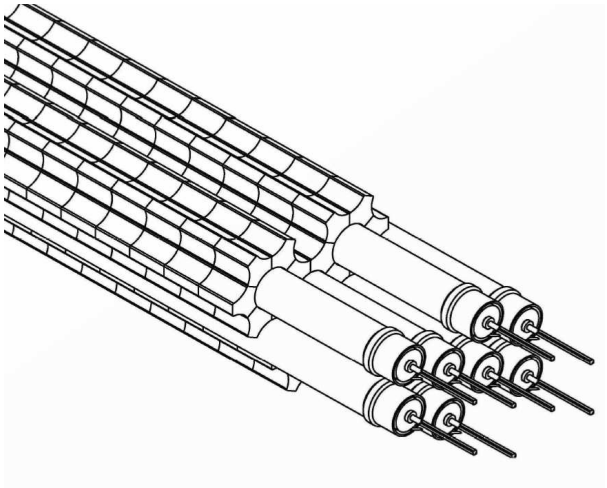

Figure 2.2: Diagram showing the arrangement of electrodes and slugs in the hadronic modules (taken from [2]).

Chapter 3

TestBeam Overview

3.1 Introduction

The testbeam studies were carried out in the H6 beamline at CERN, which is fed by the Super Proton Synchrotron (SPS). Protons from the SPS were directed at fixed targets in order to produce secondary beams of the desired particles (electrons/positrons or charged pions) at the required energy.

A diagram of the beamline is shown in figure 3.2. Beam particles emerge from the B9 magnet, traveling a distance of 32 metres and passing through several sets of instruments before reaching the FCal. The B9 magnet was used to control the vertical inclination of the beam, and thus the vertical position of the beamspot on the FCal face could be controlled via manipuilation of the currents in the B9 magnet. The cryostat containing the FCal was able to be translated horizontally and rotated, which provided control over the horizontal position of the beamspot and the angle at which the beam particles struck the front face of the calorimeter. A total of 5 beamspots were used, numbered 1,2,3, 4L and 4H. The position of these location of these beamspots is depicted in figure 3.3. Positions 1,2 and 3 were used to study the effecs of energy leakage accross the beampipe from particles impacting close to the inner diameter. High energy ($\sim$200 GeV) beams

of electrons and pions were used to provide data at these positions, and the results of these studies can be found in **??**. Position 4L was used to study the intrinsic response of the FCal with a minimal amount of material between the calorimeter and the incoming particles, whereas position 4H was used to simulate a more ATLAS-like environment with additional dead material introduced into the beamline. Electrons and pions at energies from 10-200GeV were used at these beamspots. This thesis will focus on the analysis of data taken at positions 4L and 4H, and the comparison of this data to results obtained from the Monte Carlo simulation.

3.2 Beamline Instrumentation

Eight beam profile chambers (BPCs) were used to provide tracking information on beam particles. Four of these BPCs are of a newer design, one pair of which was located about 1.6 metres downstream from the B9 magnet while the other pair was situated 3m upstream from the FCal, on an adjustable table described below. These chambers contain two readout planes, oriented at right angles such that measurements of both transverse coordinates may be made. Each readout plane covers an area of $120mm \times 120mm$, and has an average resolution of around $130\mu m$. The other four BPCs were of an older design and were able to measure a single track coordinate with a resolution of about $325\mu m$. These were positioned in the middle of the beamline (about 20m from the FCal), with two BPCs measuring the X coordinate of the beam particles and the other two the Y coordinate. In total, the eight BPCs provide six independent measurements of the X and Y coordinates of the beam particle tracks.

The adjustable was positioned about 2 metres upstream from the cryostat, on which three scintillators (S1, S2, S3) were positioned. These scintillators were polystyrene-based, and were used for triggering and beam cleaning. All three were 1 cm thick, with S1 and S2 having cross-sectional dimensions of 10cm $\times$ 10cm, while S3 had dimensions

7cm × 7cm. A veto counter was also present on the table, consisting of rectangular piece of scintillator (63cm × 63cm × 5cm) with a circular hole 65mm in diameter that the beam passed through. The height of this table could be varied such that the beam instruments were in the appropriate position for the beamspot under study.

As the liquid argon gaps in the FCal are much smaller than those used in typical liquid argon calorimeters, FCal channels are susceptible to shorts should any conductive debris find its way into the liquid argon. In order to prevent this, the FCal was housed inside a "bathtub" within the cryostat. The bathtub was made from stainless steel 1.5 mm thick, and had a rectangular shape. Holes were present on its sides to allow the liquid argon to flow in as the cryostat was filled, but these were covered with a fine mesh to keep any debris out.

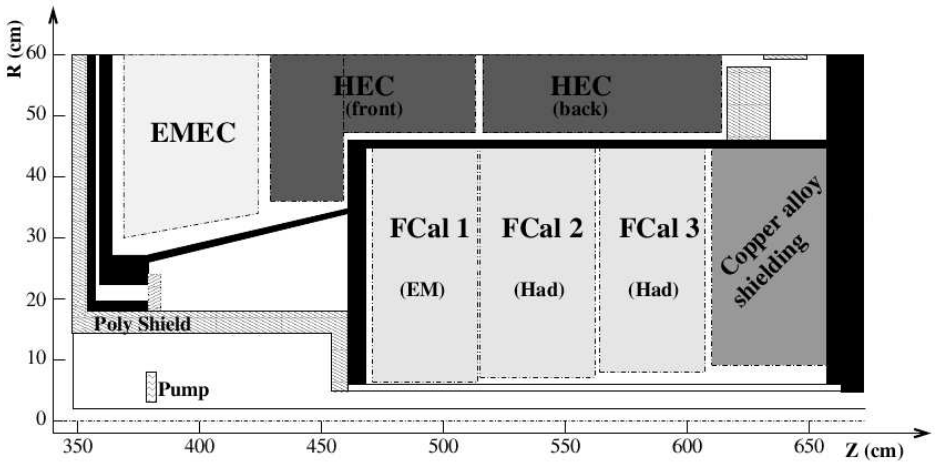

Figure 3.1: Cross section of FCal positioned within the end-cap cryostat, showing the inactive material laying between the calorimeter and the interaction point.

In order to simulate a more ATLAS-like environment for data taken at positions 1,2,3 and 4H, additional material was inserted into the beamline. A cross section of part of the ATLAS end cap is shown in figure 3.1, showing the dead material present in the detector. An aluminium plate 5.1 mm thick was bolted to the inside of the bathtub to model the cryostat bulkhead, with a slot cut out of the plate such that the additional aluminium would not effect beams directed at position 4L. The area covered by this plate is shown

in figure 3.3.

The JM shielding (labelled "poly shield" in figure 3.1) is made of boronated polyethylene and is present in ATLAS to prevent albedo radiation from scattering back into the inner detector. This was modelled in the beam test by placing a wedge shaped piece of polyethylene on the outside of the bathtub such that it covered positions 1,2, and 3, simulating the toroidal "plug" part of the shielding that lies close to the beam pipe and adjacent to the cryostat bulkhead. An iron wall was located between the adjustable table and the cryostat. This wall had a 10cm x 10cm slot cut into it to allow the beam to pass through. When taking data at position 4H, another piece of polyethylene (a rod with dimensions 10cm x 10cm x 1m) was placed at an angle in this slot. This was done in order to model the tube shaped part of the JM shielding that ran parrallel to the beam axis. When running at position 1, a small piece of aluminium was instead placed in this slot, simulating the ion pump present close to the beampipe in ATLAS.

An "excluder" made of RohaCell was also attached to the outside of the bathtub. In ATLAS the area between the FCal support tube and the beampipe is evacuated, and so the excluder was placed inside the cryostat to prevent this space from being occupied by liquid argon. The density of RohaCell is 0.011 g/cm^3 whereas that of liquid argon is 1.43 g/cm^3, so the RohaCell provides a relatively good approximation of a vacuum. An evacuated cylinder of stainless steel was also placed inside the FCal during the beam test to simulate the beampipe.

A tail-catcher calorimeter was positioned downstream of the cryostat, and was comprised of layers of steel and scintillator. Behind the tailicatcher was a beamstop of iron and concrete, and beyond that a muon counter was located. The tail-catcher and muon counter were only used for muon identification: no information from the tail-catcher was used in the analysis of the FCal response.

A CEDAR (Cerenkov Differential counter with Achromatic Ring focus, [5]) detector was located upstream of the B9 magnet and used for particle identification. Beam

particles pass through a series of chambers filled with gas (He or N_2) at high pressure, and emit cherenkov radiation at an angle that is dependant on their velocity and mass. The optics of the detector then focus this into a ring, with different types of particles producing rings of differing radii.

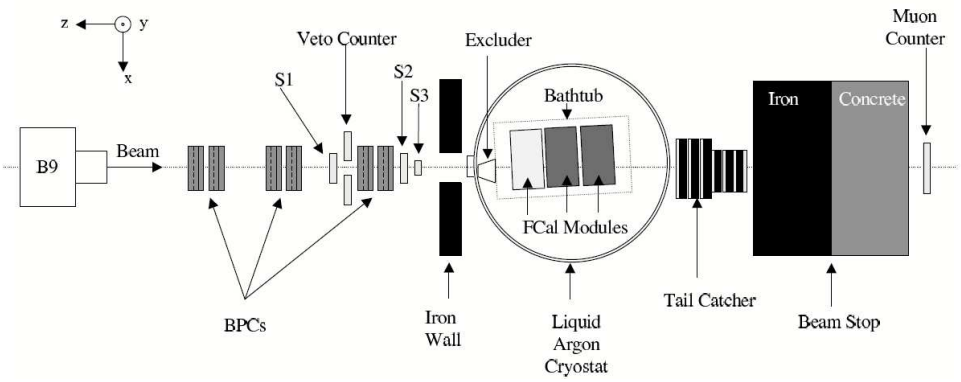

Figure 3.2: Diagram showing the setup used for the 2003 FCal beam test (not to scale).

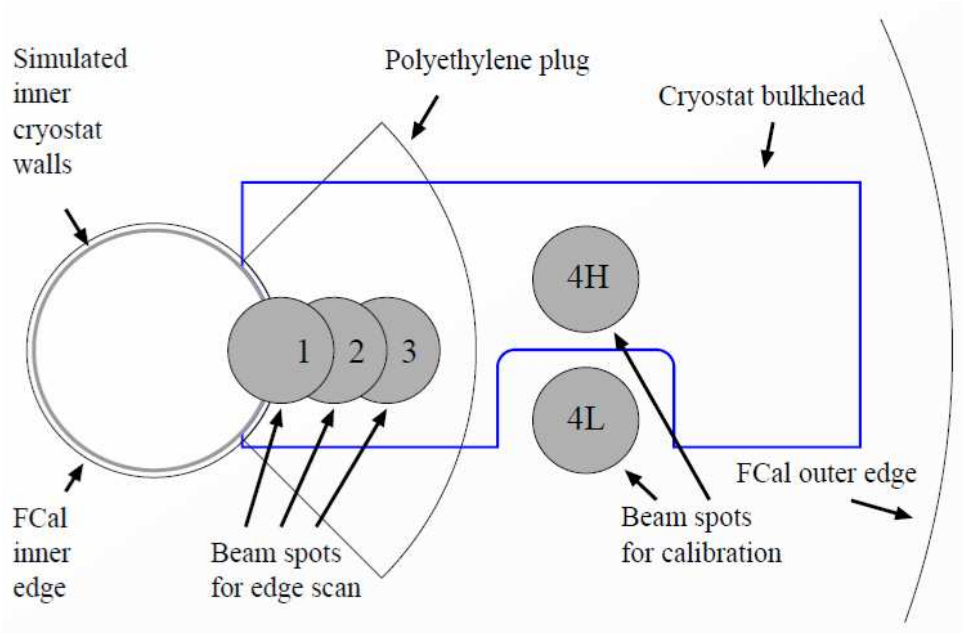

Figure 3.3: Beamspots studied in the testbeam.

3.3 FCal Electronics

An electric field of ∼1KV/mm is desired for liquid argon calorimeters. In order to provide this the rods of each electrode are supplied with high voltage while the tubes are grounded. Charge is deposited in the gap as showering particles ionize the liquid argon. The electric field in the gap then causes this charge to drift resulting in a current pulse, which is used as a signal. This pulse is triangular in shape, having a fast rise time (∼1 ns) and taking ∼61 ns to return to zero. The pulse peak is corresponds to the amount of charge deposited in the liquid argon, and is thus proportional to the amount of energy deposited in the liquid argon.

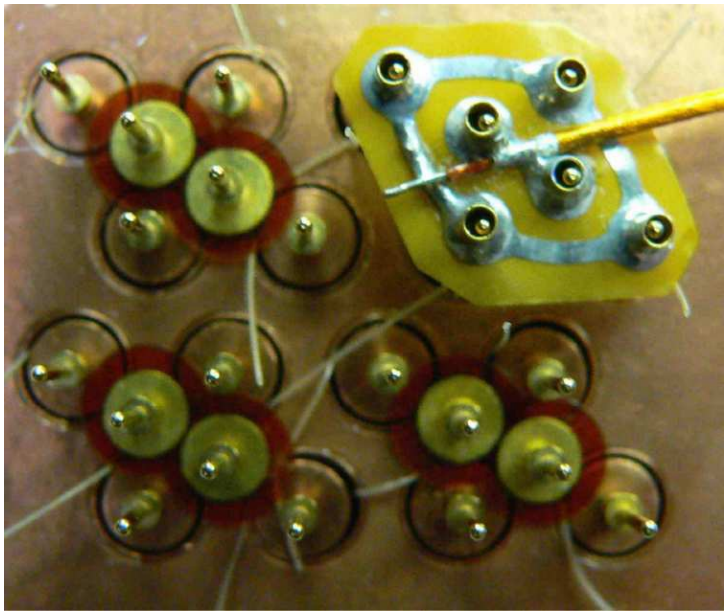

Figure 3.4: Photo of an endplate of FCal1, taken during assembly, showing the interconnect board and the coaxial cable used for HV delivery and readout. Also visible are the PEEK fibres used to keep the rods centred within the tubes (Image taken from [2]).

The signal is read out on the same line that supplies the electrodes with high voltage. Electrodes in the FCal are ganged together at interconnect boards to form "tube groups". Tube groups are formed from four electrodes in FCal1, six electrodes in FCal2, and nine electrodes in FCal3. The rods from these electrodes are connected to the interconnect

board, which is supplied with HV via a coaxial cable as shown in figure 3.4. The tubes are also grounded through this coax: each interconnect board is connected to the FCal end plate, and the tubes are inserted in such a way that they have a good electrical connection with the end plates. As the HV line supplying a tube group is also used to read out the signal, the current pulses from each electrode are summed together on the interconnect board to form one signal for the entire tube group.

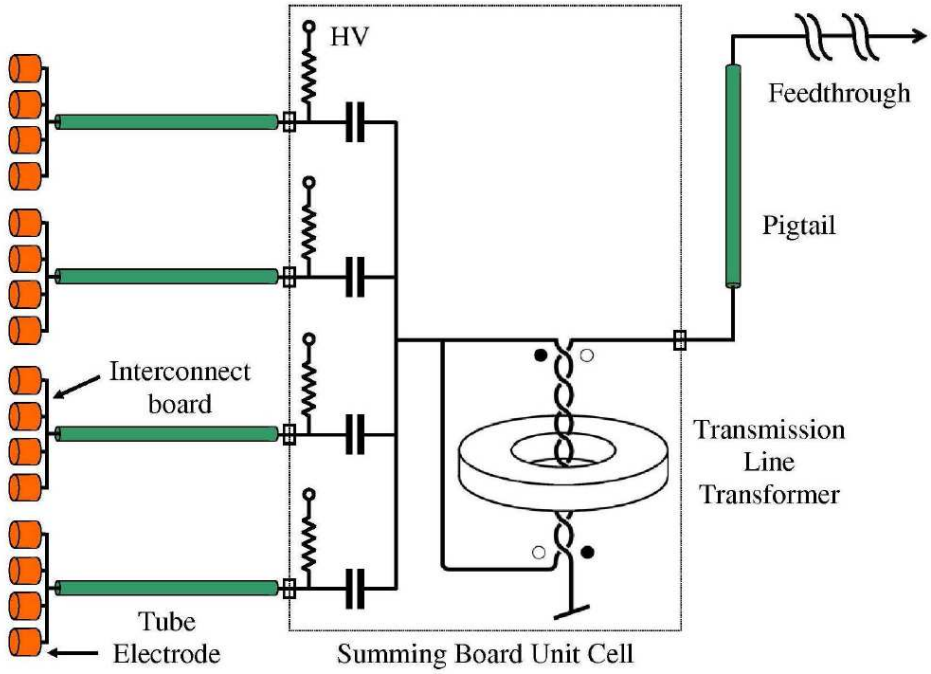

Figure 3.5: Illustration of a summing board used in the readout electronics. A single channel is composed of four tube groups, which each consist of 4/6/9 electrodes in FCal1/FCal2/FCal3.

The readout lines are then fed out to a summing board. On each summing board, four signals are again combined to form a single channel. One FCal channel thus corresponds to four tube groups, which is equivalent to 16/24/36 electrodes in FCal1/FCal2/FCal3. The summation is carried out through a transmission line transformer, which serves to match the impedence of the readout coax to that of the "pigtail" cable used to carry the signal away from the summing board (figure 3.5). A different HV source is used to

supply each tube group, so that if one source fails then the other three tube groups in the channel should still be powered. This is the case in ATLAS, where . . . .

Near the inner and outer edges of the FCal the tube groups are irregularly shaped, and it is not feasible to sum these in a coherent manner. These tube groups form the "unsummed" channels.

The summing boards are located inside the cryostat. the pigtail cables carry the signal from the summing boards out through the cryostat feedthrough to the Front End Boards (FEBs). The FEBs used during the beam test were prototypes, and had a similar design to those currently being used in ATLAS. On the FEB, the signal is preamplified and then shaped. The shaping is done in order to improve the signal to noise ratio of the pulse, and consists of one differentiation and two integration steps (CR-RC^2) resulting in a bipolar pulse shape. The pulse is also amplified at the same time it is shaped. Three different gains (low, medium, and high) are used. The amplification used for high gain is about 10 times as much as that used for medium gain, which in turn is about 10 times higher than that used for low gain.

Timing on the FEB is done by a Trigger Timing Control (TTC) chip, which emits clock pulses every 25ns. The signal (at each gain) is sampled at every 25ns, and stored (as an analog voltage) on a Switched Capacitor Array (SCA) circuit. The pulse shapes for the three FCal modules are shown in figure 3.6. Each pulse consists of an initial positive lobe followed by a longer, negative lobe, the start of which can be seen in the figure.

When a trigger signal indicates that the event should be read out, the pulse samples are read off the SCA and fed to an ADC (Analog to Digital Converter). For each sample the ADC then outputs a 12-bit signal, which is a discretized voltage capable of taking one of 4,096 distinct logical levels. Generally only a single gain is read out of the SCA and digitized, and so a gain selector chip is used to determine which gain will yield the largest pulse height without saturating the ADC output. As the pulse shape has a negative lobe,

a "pedestal" value must be subtracted from the digitised output in order to represent a negative value. To acheive this, an offset is added to the samples read from the SCA just prior to them being digitised. The offset voltage is chosen such that the pedestal value is around 1,000 ADC counts, leaving around 3,000 ADC counts to represent the positive lobe of the pulse. The pedestal value is calculated using physics data on a run by run basis. For each channel, the first sample of each pulse is averaged over the entire run, and this value is used as the pedestal during reconstruction.

3.4 Signal Reconstruction

3.4.1 Optimal Filtering method

Offline reconstruction of the energy deposited in the calorimeter is done through the use of optimal filtering coefficients (OFCs) [6]. These coefficients may be used to reconstruct the amplitude of the signal pulse and its timing in such a way that the effect of the noise on the reconstruction is minimised.

The OFC method produces two sets of coefficients, a_i and b_i, which on average correctly produce the pulse amplitude A and time shift τ:

$$A = \left\langle \sum_i a_i S_i \right\rangle \tag{3.1}$$

$$A\tau = \left\langle \sum_i b_i S_i \right\rangle, \tag{3.2}$$

where S_i is the value of the i-th signal sample, after pedestal subtraction. Given that the pulse shape, $g(t)$ is known, these samples may be expressed as

$$S_i = Ag(t_i - \tau) + n_i = Ag(t_i) - A\tau g'(t_i) + n_i, \tag{3.3}$$

where g' is the derivative of the pulse shape and n_i is the noise present in the i-th sample.

Equations 3.1 and 3.2 may then be rewritten as

$$A = \sum_i a_i A g(t_i) - a_i A \tau g'(t_i) + a_i \langle n_i \rangle \quad (3.4)$$

$$A\tau = \sum_i b_i A g(t_i) - b_i A \tau g'(t_i) + b_i \langle n_i \rangle \quad (3.5)$$

The coefficients should be chosen in such a way that the variances of A and $A\tau$ are minimised. As the mean value of the noise is zero, these variances may be written as

$$\mathrm{Var}(A) = \sum_{i,j} a_i a_j \langle n_i n_j \rangle \quad (3.6)$$

$$\mathrm{Var}(A\tau) = \sum_{i,j} b_i b_j \langle n_i n_j \rangle, \quad (3.7)$$

where $\langle n_i n_j \rangle$ is simply the autocorrelation matrix of the noise between samples. This minimisation may be carried out using the method of Lagrange multipliers, with constraints

$$\sum_i a_i g_i = 1, \qquad \sum_i a_i g'_i = 0$$

$$\sum_i b_i g_i = 0, \qquad \sum_i b_i g'_i = -1$$

obtained from equations 3.4 and 3.5.

A SPICE [10] simulation of the electronics chain is used to obtain an initial estimate of the pulse shape used in the OFC calculation. This estimate was then improved using an iterative procedure that incorporated data taken from physics runs. The data used in this procedure is taken from events in which have a large pulse amplitude, in order to ensure that the signal is coming from a physical energy deposit.

3.4.2 Timing and Pulse Shapes

Pulse samples were taken according to the TTC clock on the FEBs. Seven samples were recorded for each pulse during physics runs, with the timing adjusted such that on average the fourth sample was coincident with the pulse peak. In ATLAS the timing is

synchronised to the LHC clock, such that samples are taken in time with each bunch crossing. This was not the case during the beam test, and beam particles arrived at random phases with respect to the TTC clock. In this case, timing for the vent was taken from the S1 scintillator. A LeCroy 2228A Time to Digital Converter (TDC) with a timing resolution of 50 ps was used to measure the phase difference between the event trigger and the TTC clock, with the trigger from the S1 scintillator uised as a start signal and the clock pulse from the TTC used as a stop signal. The TDC only measured a phase difference between the start and stop signals, and so readings close to 0 or 25 ns were ambiguous. To resolve this a second TDC was used in which the stop signal was delayed by 10 ns, which allowed the time interval between the beam trigger and the TTC pulse to be determined uniquely.

While the OFC method is capable of handling time differences between pulse peaks and sample times, the taylor expansion used in equation 3.3 becomes invalid when this time, τ, becomes large. To avoid this issue, events are binned according to the TDC phase time, using 25 bins of width 1 ns. A set of OFCS is calculated for each bin using a pulse shape that has been shifted in time by the relevant amount. During event reconstruction, the amplitude of each pulse is obtained by using the set of OFCs corresponding to the TDC phase time for that event. Only a single set of OFCs is required at `ATLAS`, as in this case the TTC clocks are synchronised with that of the LHC, and so the samples are taken in time with the bunch crossings.

3.4.3 Offline Reconstruction

Offline reconstruction of testbeam data is carried out in `Athena`. For each event, the LArRawChannelBuilder algorithm retrieves the pulse samples (which are stored as LArDigits), and fetches the OFCs from a database. The pedestal is then subtracted from these samples and the OFCs are applied, giving the amplitude of the pulse in ADC counts. This amplitude is then converted to an energy using a factor (the "ADC2MeV" value)

that depends on the channel and gain. The energy of the channel, in MeV, is then stored as a LArRawChannel object. Another algorithm is then used to create CaloCell object from this LArRawChannel. From the CaloCell the position, time, energy, quality, and four-momentum of the channel may be retrieved, making CaloCells suitable objects to be used in data analysis. Because of this, CaloCell information is recorded by default in Event Summary Data (ESD) files, which are one of the standard formats used by ATLAS. CaloCells are also used as input for topoclustering algorithms, which in turn are used as input for jet-finding and missing energy algorithms.

For initial studies of the testbeam data, the ADC2MeV factors used in the reconstruction were set to 1, such that the final energies obtained were in terms of ADC counts. This was done to make life easier when measureing energy scale in FCal. However LArRawChannel class used in Athena stores channel energy as an integer number of MeV, energies less than 1 MeV are deemed insginificant. An unforeseen consequence of this was that in earlier versions of the testbeam analysis, cell energies were truncated (rounded down) to an integer number of ADC counts. This rounding meant that energy was effectively lost during the reconstruction proccess, up to ∼80 MeV per cell in FCal1 and ∼160 (∼185) MeV in FCal2 (FCal3). This had some effect on the electron results but a more significant effect on the hadron results, due to broader showers and higher ADC2MEV factors used in the hadronic modules. The bug has since been fixed, and none of the results presented here are affected by it.

flowchart

3.5 Simulation

A Monte Carlo simulation of the testbeam setup has been developed within the Athena framework. Geant 4.9.2 [**?**] is used to simulate interactions of the beam particles with beamline elements. The results of this simulation are then reconstructed and analyzed

in the same manner as the data.

3.5.1 Geant4

Geometry in Geant4 is described in terms of volumes. A "solid volume" is first created to describe the shape of a given object. This is then used to derive a logical volume, which inherits the shape of the solid and is associated with a material. A material type is defined by specifying the relative mass fractions of its constituent elements and the density of the material. Logical volumes are then used to construct physical volumes , which inherit the shape and material information from the logical volume. A physical volume also has a position and orientation assigned to it, and it is by positioning these physical volumes that the geometry of the simulation is defined. A special physical volume, the world volume, is created first. All subsequent physical volumes are then placed either inside the world, or inside another physical volume.

The description of the beamline used in the simulation contains all the beamline elements from the B9 magnet to the tailcatcher, including all scintillators, BPCs, cryostat material and beampipes. Most of these objects are defined from scratch, however the description of the FCal is taken from that used in the full ATLAS simulation while the cryostat description has been taken from another testbeam simulation. Elements upstream of the B9 magnet, such as the CEDAR detector, have not been included.

The description of the FCal has been modified in some respects, as some minor errors were found in the material description. In the default FCal definition the rods in the hadronic modules are made of WFeNi rather than tungsten, which has a slightly higher density. The density of the absorber matrix was also found to be incorrect. The correct materials and densities (given in section 2.2.1) have been used in the testbeam simulation.

The abstract way in which positions are defined can also lead to errors. Geant4 uses matrices to represent transformations, and so the order of operations are important. When a physical volume is inserted into the world (or another physical volume), it is

placed at the origin of that volume's coordinate system, and must be repositioned by applying transformations. These transformations are not commutative, so care must be taken to ensure the operations are applied in the correct order. The last operation specified prior to the creation of a physical volume is the first operation applied to it once it is placed in the world, which can be counterintuitive if these transformations are not thought of as matrix operations.

In `Geant4`, physics is defined in terms of processes. Particles are propagated through the simulation in a step by step fashion, with continuous processes (such as ionisation) acting on the particle during the step while discrete processes (such as decays, pair production) take place at the end of a step. After the step, the particle's kinematics are updated. Secondary particles are only produced if their energy exceeds a range cut. If a process would produce a secondary particle with energy less than the range cut, this energy is instead deposited in the material. Range cuts are specified as a distance, but `Geant4` converts this distance to an energy based on the material the particle is travellling through at the time. A range cut of $30\mu m$ has been used for testbeam simulations, which is appropriate given the narrow width of the active liquid argon gaps.

Electromagnetic showers are generally well understood and relatively straightforward to model. Hadronic showers are more complex, and a variety of processes are used to describe the shower development. Hadronic "physics lists" are used to define the specific set of processses available and the energy ranges in which they are used. Three physics lists have been used in the simulation of the test beam, and are outlined below:

- QGSP_BERT Quark Gluon String Precompound with Bertini cascade. This is the default physics list used for `ATLAS` simulations. The Quark Gluon String model [8] is used to simulate hard inelastic scattering for hadrons in with energies from 12 GeV to 100 TeV. One or more strings are formed between between partons of the colliding hadrons, and these strings are then "cut" by inserting quark/anti-quark pairs. One member of the pair becomes the new "end" of the string, while the

other forms a hadron with the parton that was the old end. This process repeats until the string has insifficient energy to form new pairs. The precompound model is then used to de-excite what remains of the nucleus. Between 9.5 and 25 GeV, a Low Energy Paramaterization (LEP) is used to describe inelastic scattering [7]. For particles with energy less than 10 GeV, a Bertini intra-nuclear cascade model [3, 4] is used to describe inelastic scattering with nuclei. The incoming hadron is classically scatter within the nucleus, using cross sections and angular distributions taken from experiment.

- QGSP_BERT_HP This physics list is essentially the same as QGSP_BERT, but includes high precision modeling for low energy neutrons (¡20MeV). This method relies extensively on cross sections obtained from experiment. It was reported in [11] that the high precision neutron tracking had a significant effect on the development of hadronic showers in tungsten, and so it was considered worthwhile to investigate this physics list.

- FTFP_BERT This physics list uses the Fritiof string model [1] to model high energy inelastic interactions, which is similar to the Quark-Gluon String model described above. The Fritiof model can be applied over a wide range of energies, and is used for hadrons with energies between 5 GeV and 100TeV. As with QGSP_BERT, the precompound model and Bertini cascade are also used.

3.5.2 Reconstruction of Simulation Results

The reconstruction chain used for Monte Carlo simulations is, with a few exceptions, the same as that used for reconstruction of the test beam data. In `Geant4`, when a showering particle deposits energy through ionization in a liquid argon gap, a "hit" is produced. The hit describes the size, time and location of the energy deposited in the liquid argon. A digitization step then collects these hits and simulates the electronics chain to in order

to produce digitized samples of the pulse shape, which are again stored as LArDigits. These are then processed into LArRawChannels and CaloCells in the same manner as is used for data, as shown in figure **??**.

Electronic noise is must also be modeled in the simulation. Most of this noise arises in the preamplifiers on the summing boards. Noise can be quantified by studying the rms of the pedestal values, which gives a value of of 3.2 ADC counts per sample when averaged over all channels and all runs. In addition to physics data, some randomly triggered events were recorded during data taking. The data taken by these random triggers is essentially all noise, and allows the correlations in the noise to be studied.

The default method for modeling noise in the simulation is done during the digitization step, where the autocorrelation matrix for the noise is retrieved from a database. It is then used to randomly generate the noise contributions that are added to each sample. However, during data taking the level of electronic noise present was seen to vary, as can be seen in figure 3.7. Data for different beam configurations was taken at various times, so the average noise present for runs at a specific particle/beamspot/energy differs to that for runs with another beam configuration.

To account for this, randomly triggered data taken from the same runs as the physics data is used to generate noise added into the simulation, using a procedure discussed below. This method allows different beam configurations to be reconstructed with different levels of noise, whereas the default method of generating noise lacks this functionality.

3.5.3 Noise Generation and Application

The noise added into the simulation is derived from the randomly triggered data. A covariance matrix is generated by running over the randomly triggered data taken with a specific beam configuration (e.g. 200GeV pions directed at position 4L), such that

$$M_{ij} = \frac{1}{N_{\text{events}}} \sum_{n}^{N_{\text{events}}} e_{i,n}\, e_{j,n} \tag{3.8}$$

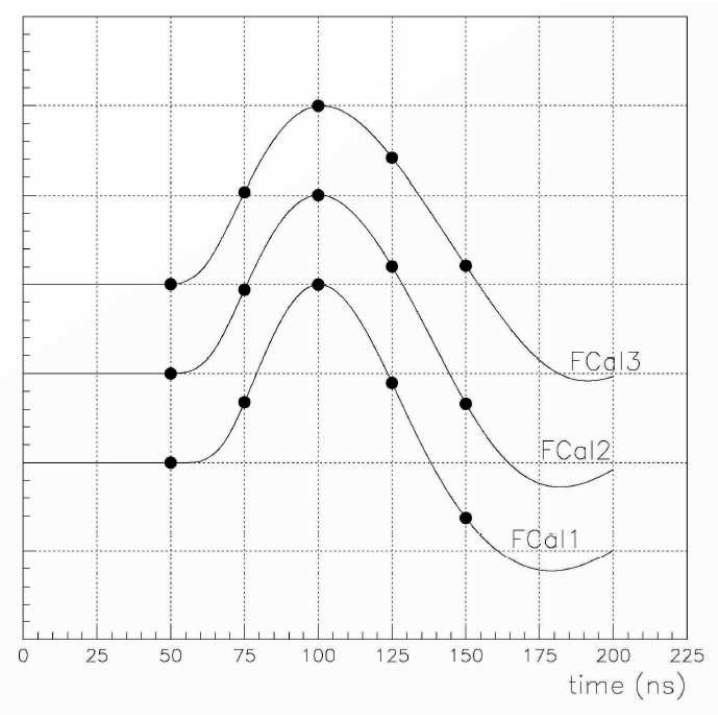

Figure 3.6: Pulse shapes for each module. The dots indicate the times at which they are sampled and digitized.

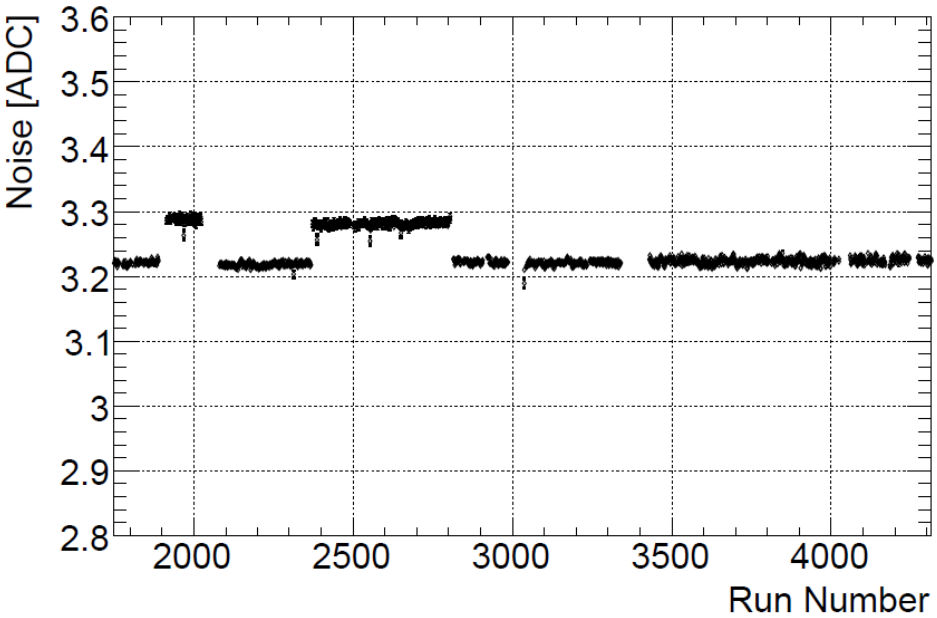

Figure 3.7: Plot showing variation in the pedestal RMS, as a function of run number. The pedestal RMS is an indication of the level of noise present in the electronics, showing that this varied with time.

where $e_{i,n}$ is the noise reconstructed from the i-th channel of the n-th event, in ADC counts. The matrix M_{ij} is then diagonalised, such that it can be written as

$$\mathbf{M} = \mathbf{U}^T \mathbf{D} \mathbf{U} \tag{3.9}$$

where $\mathbf{U}$ is a unitary matrix with columns equal to the eigenvectors of $\mathbf{M}$, and $\mathbf{D}$ is a diagonal matrix which has the eigenvalues of $\mathbf{M}$ as its entries. The matrix $\mathbf{U}^T$ thus acts as a transformation matrix, transforming information from the "channel" basis to the eigenvector basis. The eigenvectors and eigenvalues are written to file, and then retrieved during the reconstruction.

The noise is applied in the LArRawChannelBuilder algorithm, after the pulse peak has been found through application of the OFCs. The matrix U_{ij} and eigenvalues D_{ii} are first read from file. For each event a vector of noise, N_i is then generated. This is done in the eigenvector basis using a normal distribution, such that $sigma(N_i) = D_i i$. This noise is then transformed back into channel basis, such that

$$N_i' = \sum_j U_{ij} \, N_j \tag{3.10}$$

which builds in all the correlations between channels. The noise N_i' is then added to the reconstructed pulse peak of the i-th channel.

The default method relies on an autocorrelation matrix, such that a correlations between samples are present but each channel is considered independently. This method avoids dealing with the noise on individual samples and instead considers the total noise on the reconstructed pulse peak, while also incorporating correlations in noise between channels. These correlations are significant, as without them the estimations of the noise in a given cluster are too low. This is important when studying the energy resolution of the FCal, which will be discussed later.

Chapter 4

Conclusion

Bibliography

[1] B. Andersson, G. Gustafson, and B. Nilsson-Almqvist. A model for low-pt hadronic reactions with generalizations to hadron-nucleus and nucleus-nucleus collisions. *Nuclear Physics B*, 281(1-2):289 – 309, 1987.

[2] A Artamonov, D Bailey, G Blanger, M Cadabeschi, T Y Chen, V Epshteyn, P Gorbunov, K K Joo, M Khakzad, V Khovanskiy, P Krieger, P Loch, J Mayer, E Neuheimer, F G Oakham, M O'Neill, R S Orr, M Qi, J Rutherfoord, A Savine, M Schram, P Shatalov, L Shaver, M Shupe, G Stairs, V Strickland, D Tompkins, I Tsukerman, and K Vincent. The atlas forward calorimeter. *J. Instrum.*, 3:P02010, 2008.

[3] V.S. Barashenkov, H.W. Bertini, K. Chen, G. Friedlander, G.D. Harp, A.S. Iljinov, J.M. Miller, and V.D. Toneev. Medium energy intranuclear cascade calculations: a comparative study. *Nuclear Physics A*, 187(3):531 – 544, 1972.

[4] Hugo W. Bertini. Low-energy intranuclear cascade calculation. *Phys. Rev.*, 131:1801–1821, Aug 1963.

[5] Claude Bovet, Rne Maleyran, L Piemontese, Alfredo Placci, and Massimo Placidi. *The CEDAR counters for particle identification in the SPS secondary beams: a description and an operation manual*. CERN, Geneva, 1982.

[6] W.E. Cleland and E.G. Stern. Signal processing considerations for liquid ionization calorimeters in a high rate environment. *Nuclear Instruments and Methods in*

Physics Research Section A: Accelerators, Spectrometers, Detectors and Associated Equipment, 338(2-3):467 – 497, 1994.

[7] H. Fesefeldt. The simulation of hadronic showers physics and applications. Technical Report PITHA–85/02, Aachen Technische Hochschule, Germany, 1985.

[8] G Folger and J P Wellisch. String parton models in geant4. 2003.

[9] P. Krieger. Density of hadronic modules. private communication, 2007.

[10] Laurence W. Nagel and D.O. Pederson. Spice (simulation program with integrated circuit emphasis). Technical Report UCB/ERL M382, EECS Department, University of California, Berkeley, Apr 1973.

[11] P. Speckmayer. Impact of the choice of physics list on geant4 simulations of hadronic showers in tungsten. Technical Report LCD-Note-2010-00, CERN, Switzerland, 2010.